

Catalysis

Selective Reduction of CO₂ with Silanes over Platinum Nanoparticles Immobilised on a Polymeric Monolithic Support under Ambient ConditionsVijay P. Taori, Rajendar Bandari, and Michael R. Buchmeiser*^[a]

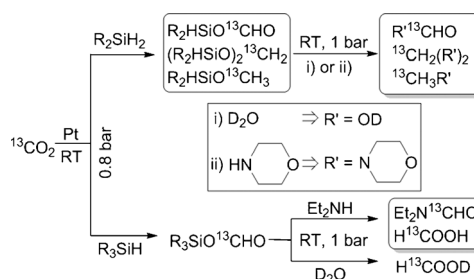
Abstract: Here, we demonstrate the use of Pt⁰ nanoparticles immobilised on a polymeric monolithic support as a ligand-free heterogeneous catalytic system for the reduction of ¹³CO₂ at room temperature and atmospheric pressure. The described system effectively reduces ¹³CO₂ with dihydrosilanes as the hydrogen source to yield a mixture of silylformates, silylacetals and methoxysilanes, which upon further hydrolysis with D₂O, produces their respective C1-type products, that is H¹³COOD, ¹³CH₂(OD)₂ and ¹³CH₃OD. If a monohydrosilane was used as the hydrogen source, a selective reduction of ¹³CO₂ to a product mixture of only silylformates was observed. Addition of diethylamine to this reaction mixture results in the formation of H¹³COOH and Et₂N¹³CHO. This robust catalytic system is not only maintenance-free and simple to handle, as compared with organometallic and organocatalyst systems, but also shows 3- to 11-fold better catalytic activity and exhibits higher turnover numbers (TONs) up to 21900 (activity = 6.22 kg_{CO₂} g_{Pt}⁻¹ bar⁻¹).

Despite the high thermodynamic stability of carbon dioxide (CO₂),^[1] its use as a C1 building block^[1e,f,2] is of ultimate interest, especially since the industrial use of C1-type chemicals occurs at very high annual volumes.^[3] CO₂ is usually used as precursor for C1-type products at high temperatures and high pressures.^[1c,3,4] Straightforward reduction of CO₂ to products with oxidation states +2 or below at low cost is therefore highly desirable and would have enormous economic and ecological impact.^[1e,f,2,5]

To this end, a limited number of studies have been carried out to achieve the reduction of CO₂ at room temperature and atmospheric pressure using either hydrosilanes^[1d,6] or hydroboranes^[1g,7] as the source of hydrogen. These studies exclusively use organocatalysts,^[2a] N-heterocyclic carbenes^[6b,8] (NHCs) or organometallic catalysts^[1g,6a,c,d,9] in solution. However,

these catalysts are usually sensitive to moisture, air and/or to solvents, which can significantly restrict their applicability. Also, the sensitivity of these catalysts does not allow for detailed characterization of the reaction mixture and only in few instances^[1g,6b,c] have the C1-type intermediates and products been characterised and reported. Also, for the purpose of recycling CO₂, Cantat and co-workers^[2a] emphasise the importance of a “diagonal approach”. This involves formation of other functional-group compounds, such as formamides, esters or tertiary amines from the intermediates of the reduced-CO₂. This approach, however, definitely requires that the catalysts used are not very sensitive towards substrates (e.g., amines) used for converting intermediates, such as formates, acetals or methyl ethers, to “derivative compounds” such as formamides or tertiary amines. In addition, the amount of catalyst required can be high,^[2a] and collectively these reasons have resulted in very low turnover numbers (TONs) of < 8300,^[1g,6a-c] with little or no possibility for the synthesis of derivative compounds based on a diagonal approach. Most of these systems also lack the ability to selectively reduce CO₂ to different C1-type intermediates upon a change in hydrogen source and show a very limited possibility for application in a continuous process.

Previously, our group has immobilised platinum and palladium on polymeric monolithic supports,^[10] the resulting heterogeneous catalysts performed well in both the continuous hydrosilylation of olefins^[10a] and in C–C coupling^[10b] reactions, showing high TONs. Here, we demonstrate the use of a Pt-loaded, polymeric monolithic support as a ligand-free catalytic system for the reduction of ¹³CO₂. As shown in Scheme 1, the use of the system with dihydrosilanes (methylphenylsilane, MPS) as a hydrogen source results in the formation of a ¹³C-labelled C1-type product mixture consisting of methoxysilanes, silylacetals and silylformates.



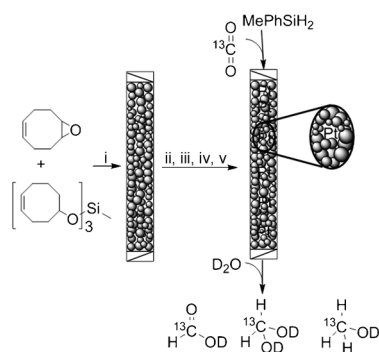
Scheme 1. Overall reaction depicting target C1 and derivative compounds.

[a] Dr. V. P. Taori, Dr. R. Bandari, Prof. M. R. Buchmeiser
Institute für Polymerchemie
Universität Stuttgart
Pfaffenwaldring 55, 70550 Stuttgart (Germany)
Fax: (+49) 711-685-64050
E-mail: michael.buchmeiser@ipoc.uni-stuttgart.de

Supporting information for this article is available on the WWW under <http://dx.doi.org/10.1002/chem.201304845>.

Notably, when this catalytic system was used with a monohydrosilane (dimethylphenylsilane, DMPS) as the hydrogen source, the selective reduction of $^{13}\text{CO}_2$ to silylformate was achieved. As outlined for numerous other catalytic systems immobilised on monolithic supports,^[11] the polymeric-monolith-based heterogenic catalytic system shown here also allows in principle for a continuous setup.

The cross-linked polymeric monolith was prepared by the ring opening metathesis polymerization (ROMP) of a *cis*-cyclooctene-based monomer and cross-linker using a 3rd-generation Grubb's catalyst. The detailed synthesis of the precursors and monolith is described in the literature^[10a,12] and in the Supporting Information. Further chemical modifications outlined in Scheme 2 were carried out to produce *vic*-diol sites. PtCl_4 was



Scheme 2. Synthesis of Pt-loaded monolith and $^{13}\text{CO}_2$ reduction with methylphenylsilane (MPS): i) $[\text{RuCl}_2(\text{pyridine})_2(\text{IMesH}_2)(\text{CHPh})]$, 2-propanol, toluene, -30°C (0.5 h), RT (16 h); ii) ethyl vinyl ether (EVE):DMSO:THF (20:40:40); iii) 0.1 N H_2SO_4 , 65°C , 24 h; iv) PtCl_4 , THF; v) 10 wt % NaBH_4 .

then introduced into the monolithic structure and reduced using NaBH_4 . The Pt^0 that formed is stabilised by both the *vic*-diol sites and double bonds present in the polymeric support (Figure 1 a). The morphology of the monolith was characterised using scanning electron microscopy (SEM, Figure 1 b), which shows the globular morphology of the monolith with globule diameters in the range of 1–2 micrometers. The specific surface area of the monolith was found to be $8.5\text{ m}^2\text{ g}^{-1}$ and an amount of $550\text{ }\mu\text{g}$ of Pt per 1 g of monolith (550 ppm) was de-

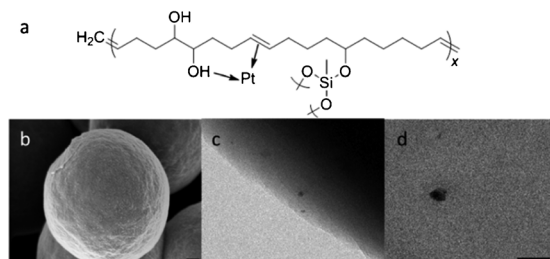


Figure 1. a) Representation of the monolithic structure and proposed coordination of Pt. b) SEM image of the monolith shows the globular morphology with diameters ranging from 1 to 2 μm . The scale bar represents 200 nm. c) TEM image of monolith prior to $^{13}\text{CO}_2$ reduction. The size of the Pt nanoparticles is around 7–10 nm. Scale bar represents 50 nm. d) TEM image of the monolith after 16 days of $^{13}\text{CO}_2$ reduction in $[\text{D}_6]\text{DMSO}$. The size of the Pt nanoparticles increased to 50 nm. Scale bar represents 200 nm.

termined by inductively coupled plasma-optical emission spectrometry (ICP-OES). Transmission electron microscopy (TEM, Figure 1 c) revealed Pt nanoparticle diameters in the range of 7 to 10 nm. In addition, ICP-OES measurements found 46 ppm inert Ru (RuO_2) contamination from the deactivated catalyst. Please refer to the Supporting Information for details.

Reduction of $^{13}\text{CO}_2$ was studied by adding 10.1 mg of crushed monolith (28.4 nmol of Pt) to an NMR tube equipped with a J. Young valve fitting. Due to its good solubility parameters for CO_2 ,^[13] $[\text{D}_6]\text{DMSO}$ (700 μL) was added to the NMR tube both as a reaction and NMR solvent and $(\text{CH}_3)\text{PhSiH}_2$ (MPS) was chosen as a hydrogen source and was added in batches to determine the activity of the catalyst. In batch I, MPS (21.5 mg, 0.176 mmol; 0.352 mmol Si–H) was added to an NMR tube (Table 1) that was then evacuated by a freeze-

Table 1. Activity of the catalyst.

Reaction time [h]	Moles of Si–H [mmol] loaded	TON ^[a,b] reacted	TOF ^[a,b] [h ⁻¹]		Integral TON ^[a,c]
			TOF ^[a,b] [h ⁻¹]	TOF ^[a,b] [h ⁻¹]	
24 ^[d]	0.352 ^[d]	0.217	7645	318	–
48 ^[d]	0.352 ^[d]	0.352	12 394	258	–
24 ^[e]	0.400 ^[e]	0.097	3409	142	–
48 ^[e]	0.400 ^[e]	0.138	4862	101	–
168 ^[e]	0.400 ^[e]	0.222	7824	47	–
336 ^[e]	0.400 ^[e]	0.270	9501	28	21 900

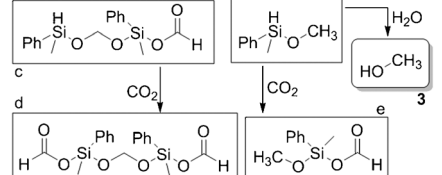
[a] Based on 28.4 nmol of Pt. [b] Based on the number of Si–H bonds reacted from either batch I or batch II. [c] Based on the total number of Si–H bonds reacted (0.622 mmol) from batch I and II. [d] Batch I. [e] Batch II. TOF = turnover frequency.

reduced using NaBH_4 . The Pt^0 that formed is stabilised by both the *vic*-diol sites and double bonds present in the polymeric support (Figure 1 a). The morphology of the monolith was characterised using scanning electron microscopy (SEM, Figure 1 b), which shows the globular morphology of the monolith with globule diameters in the range of 1–2 micrometers. The specific surface area of the monolith was found to be $8.5\text{ m}^2\text{ g}^{-1}$ and an amount of $550\text{ }\mu\text{g}$ of Pt per 1 g of monolith (550 ppm) was de-

termined by inductively coupled plasma-optical emission spectrometry (ICP-OES). Transmission electron microscopy (TEM, Figure 1 c) revealed Pt nanoparticle diameters in the range of 7 to 10 nm. In addition, ICP-OES measurements found 46 ppm inert Ru (RuO_2) contamination from the deactivated catalyst. Please refer to the Supporting Information for details.

Reduction of $^{13}\text{CO}_2$ was studied by adding 10.1 mg of crushed monolith (28.4 nmol of Pt) to an NMR tube equipped with a J. Young valve fitting. Due to its good solubility parameters for CO_2 ,^[13] $[\text{D}_6]\text{DMSO}$ (700 μL) was added to the NMR tube both as a reaction and NMR solvent and $(\text{CH}_3)\text{PhSiH}_2$ (MPS) was chosen as a hydrogen source and was added in batches to determine the activity of the catalyst. In batch I, MPS (21.5 mg, 0.176 mmol; 0.352 mmol Si–H) was added to an NMR tube (Table 1) that was then evacuated by a freeze-

As shown in Scheme 3, Pt activates $^{13}\text{CO}_2$ ^[1e,f,2b,14] which is then subjected to reduction in the presence of MPS. It is also evident from these spectra and Figure 2 (1) that new signals in



Scheme 3. Possible silylformate intermediates and formation of formic acid, methanediol and methanol from CO_2 and methylphenylsilane (MePhSiH_2 , MPS).

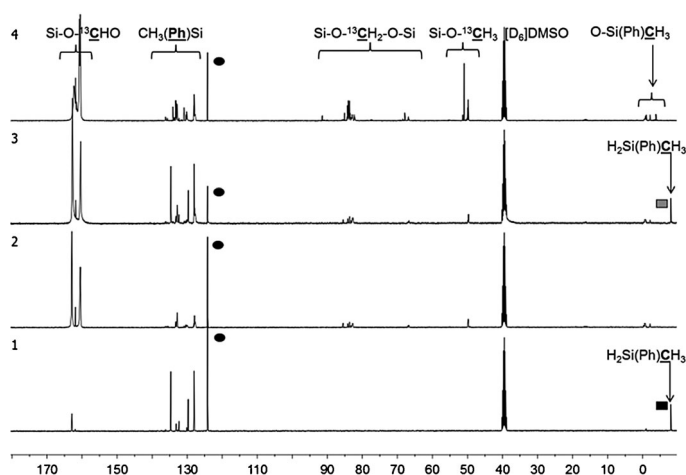


Figure 2. ^{13}C NMR spectra of the reaction mixture. 1) Spectrum acquired 10 min after the addition of $^{13}\text{CO}_2$ (●) and 0.176 mmol of MPS (batch I; ■). 2) Spectrum acquired 48 h after the addition of 0.176 mmol of MPS. 3) Spectrum acquired 1 h after the addition of 0.200 mmol of MPS (batch II; ▨). 4) Spectrum acquired 264 h after the addition of 0.200 mmol of MPS (batch II). All spectra are normalised and referenced using the solvent peak. $[\text{D}_6]\text{DMSO}$ (^{13}C : $\delta = 39.51$ ppm), $^{13}\text{CO}_2$: $\delta = 124.15$ ppm.

the region around $\delta \approx 163$ ppm form within the first 10 min (+ 30 min acquisition time) after addition of $^{13}\text{CO}_2$ to the NMR tube. Within the same time interval, a new resonance in the ^{13}C NMR spectrum evolved at $\delta = -1.0$ ppm, which represents the methyl carbon attached to the Si atom of the Si-O-species (either H-Si-O or O-Si-O) at the expense of the resonance for the methyl carbon in MPS at $\delta = -8.0$ ppm. The ^1H NMR spectrum taken after 3 h (Figure S4 in the Supporting Information) reveals the evolution of two new peaks in the formyl region. These two peaks represent a doublet centred at $\delta = 8.29$ ppm with a coupling constant $^1J_{\text{C-H}}$ of 229.6 Hz resulting from ^1H - ^{13}C coupling and thus confirm the formation of a ^{13}C -labelled silylformate as a result of the reduction of $^{13}\text{CO}_2$. The mentioned $^1J_{\text{C-H}}$ coupling constant was also verified from ^{13}C -coupled ^1H NMR spectroscopy (Figure S5) for a doublet centred at $\delta = 162.0$ ppm with a coupling constant $^1J_{\text{C-H}} = 229.6$ Hz. In principle, the formation of many different silylformate intermediates is possible (Scheme 3a–e) due to the presence of two Si–H bonds in MPS. And in fact, numerous products were observed in the ^1H NMR spectrum (Figure S6) as the silylformate peaks show significant broadening and the ^{13}C NMR spectrum shows multiple peaks evolving around $\delta \approx 162$ ppm (Figure 2, Figure S7). In the ^{13}C NMR spectrum new peaks also evolve at $\delta \approx 85$ ppm within three hours (Figure S7, 1) after the addition of $^{13}\text{CO}_2$ while after another three hours new peaks evolve at $\delta \approx 50$ ppm (Figure S7, 2) suggesting the formation of disilyloxymethane- (RPhCH_2SiO) $_2$ $^{13}\text{CH}_2$ ($\text{R} = \text{H}$, ^{13}CHO , Scheme 3c, d and g) and methoxysilyl-intermediates ($\text{RPhCH}_2\text{SiO}^{13}\text{CH}_3$, $\text{R} = \text{H}$, ^{13}CHO Scheme 3e, f).

Following the reaction by ^1H NMR spectroscopy (Figure S6 in the Supporting Information) revealed that the H–Si–H species of MPS at $\delta = 4.28$ ppm (q, $^3J_{\text{H-H}} = 4.21$ Hz, 2H; SiH $_2$) was constantly consumed over 24 h. This was further confirmed by the disappearance of the methyl shift at $\delta = -8.0$ ppm within 24 h

(Figure S7; Figure 2, 2 for 48 h). Clearly, this depletion of the hydrogen source concomitantly results in the formation of intermediates bearing the Si–O (either H–Si–O or O–Si–O) moiety. The O–Si–H moiety (Figure S9) showed up as quartets in the region $\delta = 5.10$ – 5.20 ppm with coupling constants $^3J_{\text{H-H}}$ in the range 2.75–2.97 Hz. Further acquisition as shown in Figure 2 (2) and Figure S8 (2) indicate that within 48 h, all Si–H species (H–Si–H and H–Si–O) were consumed. A negative control reaction in the absence of the monolith showed only extremely slow reduction ($\ll 0.5\%$ within 24 h, Figure S10), clearly underlining the role of Pt. After this time, only one very minor peak was observed by ^{13}C NMR spectroscopy in the silylformate region.

Next, another 25 mg (0.400 mmol Si–H) of MPS (batch II) were added at RT to the earlier-discussed reaction mixture, which was then again pressurised with $^{13}\text{CO}_2$ (0.8 bar). More prominent peaks for $\text{SiO}^{13}\text{CHO}$, $\text{SiO}^{13}\text{CH}_2\text{OSi}$ and $\text{SiO}^{13}\text{CH}_3$ intermediates were visible at the end of this reaction (Figure S11 in the Supporting Information).

Once little further reduction was observed, the intermediates were hydrolyzed by addition of 70 μL (excess) of D_2O and NMR characterization of the hydrolysis mixture was carried out after 15 h. ^1H NMR spectroscopy shows a doublet centred at $\delta = 8.12$ ppm, $^1J_{\text{C-H}} = 215.5$ Hz (Figure 3) for formic acid (H^{13}COOD). Its formation was also confirmed by ^{13}C -coupled ^1H NMR spec-

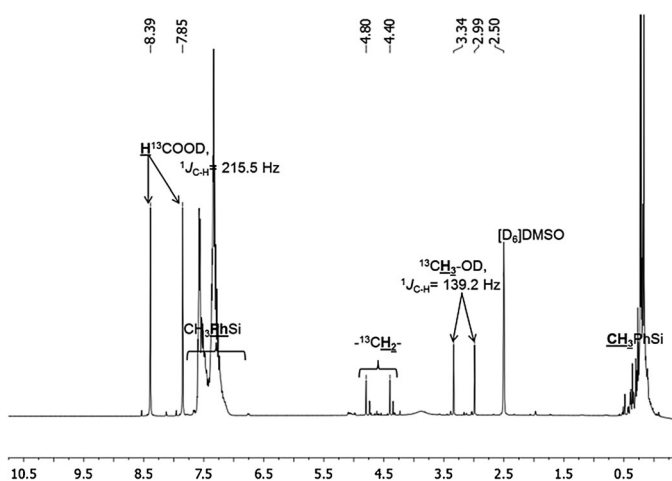


Figure 3. ^1H NMR spectrum acquired 15 h after the addition of excess of D_2O to the reaction mixture of MPS, $^{13}\text{CO}_2$ and Pt-loaded monolith. The spectrum is referenced using the solvent peak. $[\text{D}_6]\text{DMSO}$ (^1H : $\delta = 2.50$ ppm).

troscopy (Figure 4), which shows a doublet at $\delta = 163.3$ ppm, $^1J_{\text{C-H}} = 215.5$ Hz. Methanol ($^{13}\text{CH}_3\text{OD}$) showed up as a doublet centred at $\delta = 3.16$ ppm, $^1J_{\text{C-H}} = 139.2$ Hz (Figure 3) and was further confirmed by a quartet centred at $\delta = 4.88$ ppm, $^1J_{\text{C-H}} = 139.2$ Hz (Figure 4). Again, $1 \leq x \leq 3$ in $^{13}\text{CH}_x$ stated here was validated by ^{13}C -coupled ^1H NMR spectroscopy (Figure 3). In Figure 3, hydrolysis products of silyl acetal-type intermediates are visible as doublets centred around $\delta = 4.60$ ppm ($J \approx 158.9$ Hz) which can also be seen in Figure 4 as triplets in the range of $65 < \delta < 85$ ppm. These triplets confirm the pres-

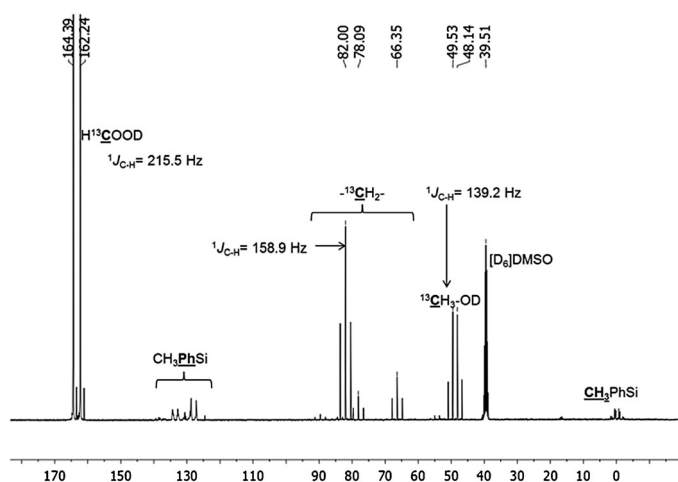


Figure 4. ^{13}C -coupled ^1H NMR spectrum acquired after the addition of excess of D_2O to the reaction mixture of MPS, $^{13}\text{CO}_2$ and Pt-loaded monolith. The spectrum is referenced using the solvent peak. $[\text{D}_6]\text{DMSO}$ (^{13}C : $\delta = 39.51$ ppm).

ence of different $^{-13}\text{CH}_2-$ motifs. Although the exact analysis of these compounds is beyond the scope of this study, we suspect the formation of methandiol as one of the major products.

As shown in Table 1, the heterogeneous catalyst shows high activity with TONs of about 12400 within 48 h (TOF = 258 h^{-1} , batch I, based on the consumption of the Si–H bond). Upon addition of further MPS and $^{13}\text{CO}_2$, the TOF decreased to 28 h^{-1} within 16 days. This is attributed to the growth of the Pt nanoparticles due to Ostwald ripening, a common phenomenon observed with metallic nanoscale systems.^[10a,15] In fact, TEM images of the monolith acquired after its use in the reduction reaction (Figure 1, d) revealed an increase in size of the Pt nanoparticles from about 7 nm to about 50 nm. Notably, the overall TON obtained in this reaction was around about 21 900 (activity = $6.22\text{ kg}_{\text{CO}_2}\text{g}_{\text{Pt}}^{-1}\text{bar}^{-1}$), which is 3- to 11-fold higher than reported TONs,^[19,6a-c] even though the entire reaction was carried out at room temperature and a very low pressure of 0.8 bar.

When CO_2 -reduction was carried out with a monohydrosilane, that is, with dimethylphenylsilane (DMPS), dimethylphenylsilyl formate (Figure S13 in the Supporting Information) formed selectively. The reaction was also carried in $[\text{D}_7]\text{DMF}$ and was found to proceed faster than in DMSO. Upon termination of this reaction with excess of diethylamine, ^{13}C NMR spectroscopy provided clear evidence for the formation of diethylformamide ($\delta = 162.5$ ppm) and formic acid ($\delta = 167.7$ ppm) (Figure 5 and Figure S17). GC-MS data confirm the formation of a siloxane compound (Figure S14) and of ^{13}C -labelled DEF (Figure S15). Thus, a commercially available sample of DEF showed exactly the same retention time and identical fragmentation (Figure S16). A similar reaction pathway as with DMPS was observed when excess morpholine was added to the reaction mixture containing $^{13}\text{CO}_2$, MPS and the Pt-loaded monolith in $[\text{D}_6]\text{DMSO}$. Formation of ^{13}C -labelled 4-formylmorpholine, bis(4-dimorpholinyl)methane and N-methylmorpholine

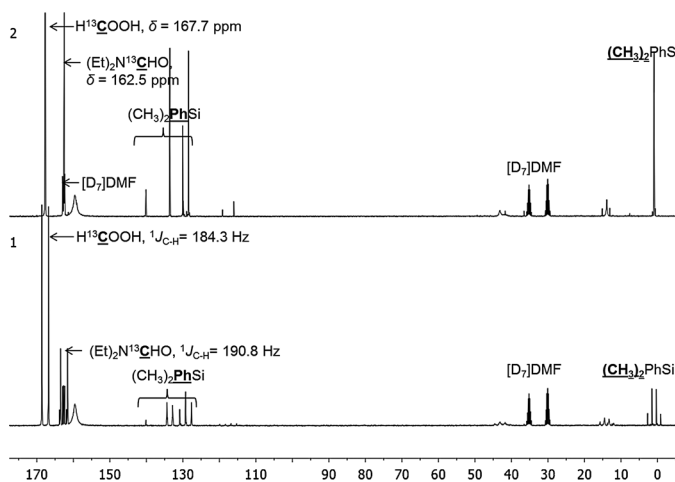


Figure 5. ^{13}C NMR spectra acquired after the addition of excess of diethylamine to the reaction mixture containing DMPS $^{13}\text{CO}_2$ and Pt-loaded monolith. 1) ^{13}C -coupled ^1H NMR spectrum, 2) ^{13}C NMR spectrum. Spectra are normalised and referenced using the solvent peak. $[\text{D}_7]\text{DMF}$ (^{13}C : $\delta = 30.1$ ppm).

was confirmed by comparison with commercially available compounds (Figure S18–S24).

In summary, the system reported here shows high activity for the reduction of $^{13}\text{CO}_2$ and allows for the synthesis of C1-type products such as $^{13}\text{CH}_3\text{OD}$, H^{13}COOD and formamides and other derivative compounds. With a monohydrosilane, selective formation of silylformates is achieved. Notably, the absence of any ligand in this heterogeneous-type catalyst offers access to a simple and continuous setup reducing the woes for separation and strengthening the concept of “diagonal approach”^[2a] for CO_2 recycling. Studies to immobilise bimetallic Pt alloys for the heterolytic splitting of H_2 as a source of hydrogen for CO_2 reduction are underway.

Acknowledgements

The authors wish to thank PD Dr. Michael Schweikert, Biologisches Institut - Abteilung Zoologie, Universität Stuttgart, for TEM measurements.

Keywords: carbon dioxide · monolith · platinum · reduction · silanes

- [1] a) F. Goettmann, A. Thomas, M. Antonietti, *Angew. Chem.* **2007**, *119*, 2773–2776; *Angew. Chem. Int. Ed.* **2007**, *46*, 2717–2720; b) S. Wesselbaum, U. Hintermair, W. Leitner, *Angew. Chem.* **2012**, *124*, 8713–8716; *Angew. Chem. Int. Ed.* **2012**, *51*, 8585–8588; c) T. J. Schmeier, G. E. Döbereiner, R. H. Crabtree, N. Hazari, *J. Am. Chem. Soc.* **2011**, *133*, 9274–9277; d) Y. Jiang, O. Blacque, T. Fox, H. Berke, *J. Am. Chem. Soc.* **2013**, *135*, 7751–7760; e) M. Aresta, A. Dibenedetto, *Dalton Trans.* **2007**, 2975–2992; f) M. Cokoja, C. Bruckmeier, B. Rieger, W. A. Herrmann, F. E. Kühn, *Angew. Chem.* **2011**, *123*, 8662–8690; *Angew. Chem. Int. Ed.* **2011**, *50*, 8510–8537; g) S. Chakraborty, J. Zhang, J. A. Krause, H. Guan, *J. Am. Chem. Soc.* **2010**, *132*, 8872–8873.
- [2] a) C. D. N. Gomes, O. Jacquet, C. Villiers, P. Thuéry, M. Ephritikhine, T. Cantat, *Angew. Chem.* **2012**, *124*, 191–194; *Angew. Chem. Int. Ed.* **2012**, *51*, 187–190; b) K. Huang, C.-L. Sun, Z.-J. Shi, *Chem. Soc. Rev.* **2011**, *40*, 2435–2452.

- [3] T. Schaub, R. A. Paciello, *Angew. Chem.* **2011**, *123*, 7416–7420; *Angew. Chem. Int. Ed.* **2011**, *50*, 7278–7282.
- [4] K. Tominaga, Y. Sasaki, M. Kawai, T. Watanabe, M. Saito, *J. Chem. Soc. Chem. Commun.* **1993**, 629–631.
- [5] W. Leitner, *Angew. Chem.* **1995**, *107*, 2391–2405; *Angew. Chem. Int. Ed. Engl.* **1995**, *34*, 2207–2221.
- [6] a) S. Park, D. Bezier, M. Brookhart, *J. Am. Chem. Soc.* **2012**, *134*, 11404–11407; b) S. N. Riduan, Y. Zhang, J. Y. Ying, *Angew. Chem.* **2009**, *121*, 3372–3375; *Angew. Chem. Int. Ed.* **2009**, *48*, 3322–3325; c) T. Matsuo, H. Kawaguchi, *J. Am. Chem. Soc.* **2006**, *128*, 12362–12363; d) A. Jansen, S. Pitter, *J. Mol. Catal. A* **2004**, *217*, 41–45.
- [7] M.-A. Courtemanche, M.-A. Légaré, L. Maron, F.-G. Fontaine, *J. Am. Chem. Soc.* **2013**, *135*, 9326–9329.
- [8] S. N. Riduan, J. Y. Ying, Y. G. Zhang, *ChemCatChem* **2013**, *5*, 1490–1496.
- [9] a) T. C. Eisenschmid, R. Eisenberg, *Organometallics* **1989**, *8*, 1822–1824; b) G. Menard, D. W. Stephan, *J. Am. Chem. Soc.* **2010**, *132*, 1796–1797; c) R. Shintani, K. Nozaki, *Organometallics* **2013**, *32*, 2459–2462; d) M. Khandelwal, R. J. Wehmschulte, *Angew. Chem.* **2012**, *124*, 7435–7439; *Angew. Chem. Int. Ed.* **2012**, *51*, 7323–7326.
- [10] a) R. Bandari, M. R. Buchmeiser, *Catal. Sci. Technol.* **2012**, *2*, 220–226; b) R. Bandari, T. Höche, A. Prager, K. Dirnberger, M. R. Buchmeiser, *Chem. Eur. J.* **2010**, *16*, 4650–4658.
- [11] a) M. R. Buchmeiser, *Chem. Rev.* **2009**, *109*, 303–321; b) E. B. Anderson, M. R. Buchmeiser, *ChemCatChem* **2012**, *4*, 30–44.
- [12] R. Bandari, A. Prager-Duschke, C. Kühnel, U. Decker, B. Schlemmer, M. R. Buchmeiser, *Macromolecules* **2006**, *39*, 5222–5229.
- [13] S. T. Perisanu, *J. Solution Chem.* **2001**, *30*, 183–192.
- [14] a) D. H. Gibson, *Chem. Rev.* **1996**, *96*, 2063–2095; b) D. A. Palmer, R. Vanelidik, *Chem. Rev.* **1983**, *83*, 651–731.
- [15] a) M. S. Wilson, F. H. Garzon, K. E. Sickafus, S. Gottesfeld, *J. Electrochem. Soc.* **1993**, *140*, 2872–2877; b) C. G. Granqvist, R. A. Buhrman, *J. Catal.* **1976**, *42*, 477–479; c) G. A. Gruver, R. F. Pascoe, H. R. Kunz, *J. Electrochem. Soc.* **1980**, *127*, 1219–1224; d) A. Honji, T. Mori, K. Tamura, Y. Hishinuma, *J. Electrochem. Soc.* **1988**, *135*, 355–359.

Received: December 11, 2013

Published online on February 19, 2014